RSC Sustainability

ROYAL SOCIETY OF CHEMISTRY

PAPER

View Article Online
View Journal | View Issue

Cite this: *RSC Sustainability*, 2025, **3**, 4746

Fe(MIL-53) metal–organic framework as a facile and sustainable Lewis acidic catalyst for the one-pot synthesis of xanthene derivatives

Ganesapandian Latha, [ab] Natarajan Saravanakumar, [a] Nainamalai Devarajan, [a] Kamaraj Shivaranjan[a] and Palaniswamy Suresh *[a]

The catalytic application of the easily preparable Fe(MIL-53) MOF was demonstrated as a sustainable solid Lewis acidic catalyst in synthesising pharmaceutically essential xanthenes under mild conditions. The Fe(MIL-53) MOF catalyst was synthesised and characterised using various analytical tools such as PXRD, FTIR, SEM, TGA and ICP-OES. The presence of a high concentration of coordinatively unsaturated Fe^{3+} sites in Fe(MIL-53) can efficiently catalyse the formation of xanthenes in the presence of a catalytic amount (1.36 mg) of MOF using environmentally friendly, non-toxic and renewable ethanol as the medium. A series of substituted xanthenes were synthesised in good to excellent yield with wide functional group tolerance. The present methodology avoids the usage of any strong reagents and uses stoichiometric amounts of the catalyst. The catalytic comparison studies with other homogeneous and heterogeneous catalytic systems proved the efficiency of the present Fe(MIL-53) MOF catalyst. The hot-filtration test and reusability profile prove the stability and sustainability of this catalyst, which were also supported by PXRD, FTIR and SEM analysis of the reused catalyst.

Received 17th March 2025
Accepted 6th August 2025

DOI: 10.1039/d5su00191a

rsc.li/rscsus

Sustainability spotlight

Iron is one of the most abundant metals in nature, and iron-based metal–organic frameworks (MOFs) have garnered significant attention due to their remarkable reactivity, stability, ease of handling, relatively low toxicity, and environmental friendliness while being cost-effective. Earlier-generation catalysts were largely based on precious metals, often homogeneous, and suffered from significant recyclability challenges. Xanthenes are a crucial class of organic compounds with diverse pharmacological properties. However, their synthesis presents challenges, particularly due to their acid-sensitive groups. The use of iron-based MOFs offers a sustainable approach to overcoming these limitations. This work aligns with the United Nations Sustainable Development Goals (SDGs) 7 and 12, which emphasize affordable and clean energy as well as sustainable consumption and production patterns, promoting a more environmentally responsible approach to catalysis.

1. Introduction

Xanthenes are an important class of organic compounds with several pharmacological properties, such as anti-coagulant, spasmolytic, anticancer, antiviral, anti-inflammatory, antibacterial, antifungal, antiproliferative, antioxidant, and specific IK_{Ca} channel blocking activities.[1–7] These compounds were widely used as synthetic precursors for many valuable organic compounds,[8] dyes,[9] and photoactive materials[10] and in laser technologies[11] and fluorescent materials for the visualisation of biomolecules[12] and detection of metal ions.[13] Tetraketones and their tautomeric enol forms are also considered to be important biologically active compounds, being assessed as tyrosinase inhibitors, and also leading intermediates in the preparation of fused heterocyclic systems such as xanthendione, acridindione and 4*H*-1-benzopyran derivatives.[14] Xanthene derivatives can be prepared generally *via* the condensation between aldehydes and 1,3-dicarbonyl compounds. To obtain xanthenes, this type of condensation reactions has been reported in the literature using homogeneous catalysts, including protonic acids,[15] Lewis acids such as $InCl_3 \cdot 4H_2O$,[16] indium triflate,[17] $FeCl_3 \cdot 8H_2O$,[18] $CuCl_2$,[19] and $NaHSO_4$,[20] and heterogeneous catalysts, such as Dowex-50W,[21] polyaniline *p*-toluenesulfonate,[22] *p*-toluenesulfonic acid,[23] sulfamic acid@MCM-41,[24] PPA–SiO_2,[25] TiO_2/SO_4,[26] nano-Fe_3O_4–TiO_2–SO_3H,[27] Fe_3O_4@NFC@NNSM-Mn(III),[28] Fe_3O_4@SiO_2@APTES@ MPIB-Mn(II),[29] TMP-PECH-COOH,[30] $CuCeO_2$ NPs,[31] ZrO_2 NPs,[32] Fe_3O_4 NPs,[33] Cu(II) NPs,[34] CuS quantum dots,[35] and Amberlyst-15.[36] In general, heterogeneous solid acid catalysts have more advantages over homogeneous acid catalysts as they can be easily recovered from the reaction mixture by simple filtration and can be reused several times

[a]*Supramolecular and Catalysis Lab, Dept. of Natural Products Chemistry, School of Chemistry, Madurai Kamaraj University, Madurai-625021, Tamil Nadu, India. E-mail: suresh.chem@mkuniversity.ac.in; ghemistry@gmail.com*

[b]*Department of Chemistry, Sethu Institute of Technology, Virudhunagar-626115, Tamil Nadu, India*

without loss of their active sites, thereby making the process more economically and environmentally feasible.[37]

Metal–organic frameworks (MOFs) are of immense interest as a new class of synthetic porous materials in various applications.[38] MOFs contain coordinatively unsaturated metal centres/sites (CUS), which act as Lewis acidic centres,[39] or functionalities suspended on their organic linkers, which act as either Brønsted basic[40] or acidic[40b,c,41] sites, promoting sustainable catalytic processes. The combination of abundant metal content and porosity makes MOFs promising heterogeneous catalysts for several organic transformations.[42] Besides the field of catalysis, due to their fascinating features, which include structural diversity, flexibility and alterability, intrinsic porosity, and desirable chemical functionality, MOFs have been used in diverse fields such as gas storage and separation, sensors, drug delivery and bioimaging.[43]

Among the reported popular MOFs, iron-based organic frameworks have attracted considerable attention[44] owing to their remarkable reactivity, stability, ease of handling, relatively non-toxic and environment-friendly nature, and low cost. Various iron-based MOFs such as Fe(BTC),[45] Fe(MIL-100),[46] Fe(MIL-53),[47] Fe(MIL-101),[48] NH_2-MIL-101(Fe),[49] MOF-235,[50] $Fe_3O(BDC)_3$,[51] $Fe_3O(BPDC)_3$,[52] and VNU-20 (ref. 53) have been used for different applications. Amongst them, Fe(MIL-53) MOF is a reliable iron-MOF that is explicitly used in photocatalysis,[55] sensors,[56] drug delivery,[54] *etc*. Centred in the middle of the d-block elements and able to support formal oxidation states varying from −II to +VI, iron-based catalysts can be widely applied in the field of organic synthesis. Iron-based metal–organic frameworks show comparable or superior catalytic activity, along with improved stability and sustainability, when used as catalysts for organic transformations. Further, the Lewis acidity of iron varies from fairly modest to very high, and this property is strongly associated with its oxidation state, and hence tunable not only based on the choice of ligands. However, although Fe(MIL-53) MOF possesses promising characteristics for catalysis such as high porosity, thermal stability, and Lewis acidic sites, its application as a heterogeneous catalyst in organic synthesis has been relatively underexplored. To date, only a limited number of organic transformations has been reported using Fe(MIL-53), including Fenton-type oxidation[57] and the synthesis of heterocyclic frameworks such as pyrano [2,3-c]pyrazoles,[58] 2-aryl-1H-benzimidazoles,[59] and pyrimido [4,5-*d*]pyrimidine derivatives.[60] In contrast, other Fe-based MOFs, such as Fe-BTC and Fe-MOF-74, have been more widely studied for diverse catalytic applications. However, to our knowledge, there have been no reports on the iron-MOF-catalysed synthesis of xanthenes *via* condensation reactions. Therefore, our current study offers a novel contribution by demonstrating the efficiency of Fe(MIL-53) MOF in catalysing the synthesis of xanthenes, further expanding its catalytic utility in organic transformations.

2. Results and discussion

In this study, we aim to explore the catalytic efficiency of Fe(MIL-53) MOF as a heterogeneous iron catalyst for synthetic organic applications. Specifically, we have utilized this catalyst for the synthesis of pharmaceutically active xanthene molecules. The Fe(MIL-53) MOF was synthesised and systematically characterised using various spectroscopic and microscopy techniques. The FTIR (Fig. 7) and PXRD (Fig. 8) analyses confirmed the formation Fe(MIL-53) as a framework, not as a coordination polymer. Further, the crystalline nature of the synthesised Fe(MIL-53) MOF (**1**) was proven by the SEM analysis, which showed the formation of highly crystalline rod-shaped Fe (MIL-53) (Fig. 9). After confirming the structure of the prepared MOF (**1**), it was used as a solid Lewis acid catalyst for the synthesis of xanthene from benzaldehyde (**2**) and dimedone (**3**) as model substrates. To obtain the optimum reaction conditions, the catalytic reaction parameters such as solvent, time, temperature and catalyst loading were screened. When employing MOFs as catalysts in heterocyclic synthesis, owing to the presence of multiple catalytic sites within their pores, the role of solvent is highly inevitable. In the present study, a spectrum of non-polar solvents was screened using 20 wt% of the Fe(MIL-53) MOF catalyst (Table 1) at the reflux temperature of the respective solvent and arbitrarily fixing 3 h as the reaction time.

The analysis of the solvent screening results clearly reveals that the solvent played a notable role in the formation of the product. In general, MOF catalysts are not more compatible with non-polar solvents. This behaviour was reflected in the present study. When non-polar solvents like toluene, dichloromethane, and dichloroethane were employed as the solvent, a moderate yield (64–72%) was observed. Meanwhile, polar solvents such as tetrahydrofuran, chloroform, 1,4-dioxane, acetonitrile and DMF resulted in moderate to good

Table 1 Solvent optimisation for Fe(MIL-53) MOF-catalysed synthesis of xanthene (**4a**)[a]

S. no.	Solvent	Yield[b] (%)
1	Methanol	85
2	Ethanol	98
3	IPA	89
4	Dioxane	80
5	ACN	58
6	DMF	88[c]
7	Toluene	64[c]
8	THF	82
9	$CHCl_3$	74
10	Water	23[d]
11	DCM	72
12	DCE	70

[a] Reaction conditions: benzaldehyde (0.71 mmol, 1.0 eq.), dimedone (1.42 mmol, 2.0 eq.), Fe(MIL-53) (25 wt%), solvent (2 mL), reflux, 3 h. [b] Isolated yield. [c] 100 °C. [d] MOF catalyst decomposed.

yield (74–88%). Conversely, in protic polar solvents such as methanol, ethanol, and isopropanol, the reaction proceeds smoothly and yields good to excellent (85–98%). Further, to explore the greener aspects, water was employed as the solvent; however, the result was not encouraging, giving a lower yield of 45% and revealing that the MOF catalyst was not stable at the end of the reaction (refer to SI, Fig. S54).

According to the overall analysis of the solvent screening results, the readily available and renewable ethanol was identified as the optimum reaction medium for the Fe(MIL-53) (**1**)-catalysed synthesis of xanthene (**4a**). Compared to the other solvent systems, in recent days, ethanol was found to be a benign reaction medium[61] owing to its renewable and non-toxic nature; besides, it is cheap and readily available.

In the present synthesis of xanthene (**4a**), temperature plays a crucial role, as inferred from the solvent optimisation. During the solvent screening, most of the solvents were used at their boiling point. The optimised ethanol was also used at its boiling point; however, to find the optimum temperature, the reactions were carried out at different temperatures.

The product yield fluctuated while tuning the temperature (Fig. 1). Initially, at room temperature, an inferior product (<2%) was noted. When the temperature increased, an enhancement in yield was observed (Fig. 1) and it increased proportionally with temperature. When the temperature reached 60 °C and 70 °C, it offered a reasonable yield (75% and 83%, respectively); however, complete conversion and the expected yield were not achieved. Further, the reaction temperature increased up to the reflux temperature of the solvent (at the boiling point of 80 °C) and gave the maximum yield (98%). To investigate the reaction at 90 °C, a sealed vessel was used to prevent solvent loss. The yield obtained under this condition did not influence the yield and gave the maximum yield of 98%. According to the temperature optimisation study, the reflux condition (80 °C) was fixed as the optimum temperature.

In heterogeneous catalysis, time optimisation is another important factor that determines the efficiency of catalysts. In the present reaction, the reaction was performed for 3 h for the initial screening of the catalyst. With the optimised solvent and temperature, the actual time required to attain the maximum yield was studied by monitoring the reaction conversion at certain intervals. Only 58% of product formation was observed after 30 min of reaction (Fig. 2). Further studied reactions after 60 min, 90 min and 120 min showed 75%, 84% and 98% yield, respectively. After 120 min and further allowing the reaction to proceed for an additional 60 min, no notable enhancement in the yield was observed. According to the above-mentioned results, 120 min (2 h) is sufficient for the complete conversion of the reactant and to achieve the maximum product (**4a**, 98%). Hence, 120 min (2 h) was fixed as the optimised time for the Fe(MIL-53) (**1**) MOF-catalysed synthesis of xanthene (**4a**).

After optimising the solvent, time and temperature, another crucial parameter, the exact quantity of catalyst required for the maximum product formation, was screened. In heterogeneous catalysis, the amount of catalyst used determines the efficiency and endorses the greener nature of the catalyst.

In the initial optimisation studies, 25 mg of the Fe(MIL-53) MOF (**1**) catalyst was employed; however, further screening started with 5% catalyst load, which resulted in moderate (70%) product (**4a**) formation (Fig. 3). Further, to identify the appropriate catalyst loading, the amount of catalyst was increased from 5% to 30 wt% and the isolated yield was calculated with an increase in the catalyst load in every additional 5% load. The screening results showed that 20 wt% catalyst loading provides the maximum yield of 98%. Further increasing the catalyst load to 25 and 30 wt% showed no remarkable improvement. This screening study demonstrated that 20 wt% of Fe(MIL-53) (**1**) catalyst load is adequate to get the maximum yield of xanthene (**4a**).

All the above-mentioned preliminary screening studies disclosed that Fe(MIL-53) (**1**) acts as an efficient heterogeneous catalyst for the synthesis of xanthene (**4a**) with 20 wt% (1.36 mg of Fe, 0.0243 mmol) of catalyst in renewable ethanolic medium

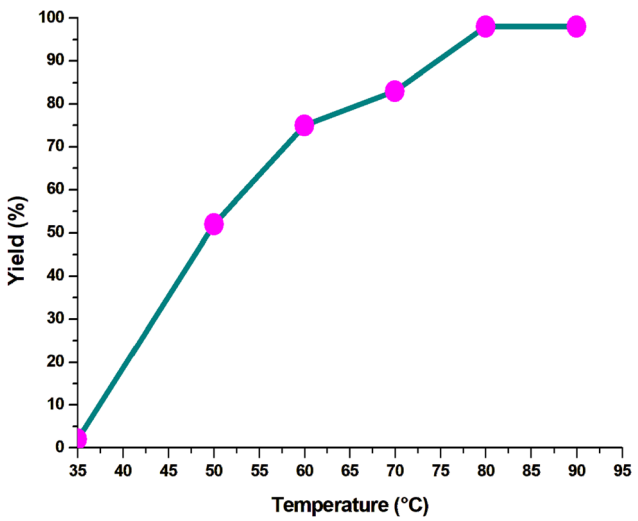

Fig. 1 Temperature optimisation for Fe(MIL-53) MOF-catalysed synthesis of xanthene (**4a**).

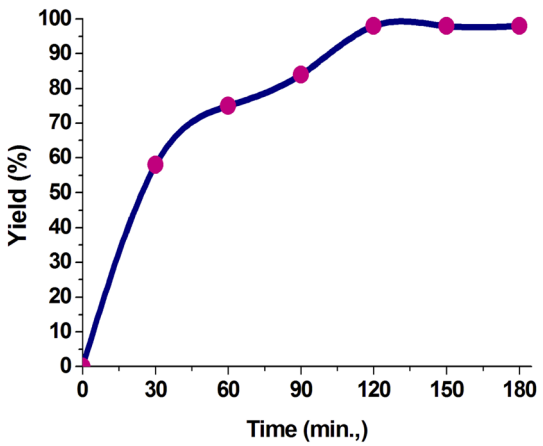

Fig. 2 Time optimisation for Fe(MIL-53) MOF (**1**)-catalysed synthesis of xanthene (**4a**).

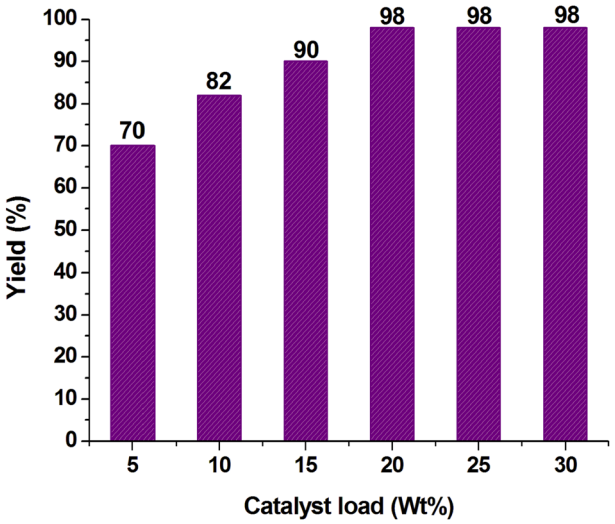

Fig. 3 Optimisation of catalyst (Fe(MIL-53) (**1**)) load for the synthesis of xanthene (**4a**).

under reflux conditions. With this mild and the reliable optimised reaction conditions in hand, to further unlock the potential of this catalyst for the synthesis of xanthene, its scope was extended to various aldehydes under the above-optimised condition, and the results are depicted in Table 2. Under the optimised reaction conditions, a series of aldehydes with different electronic natures was reacted with dimedone in the presence of 20 wt% of Fe(MIL-53) (**1**) as the catalyst in ethanolic medium. All the studied aryl aldehydes gave the respective xanthenes in good to excellent yield, and the products are presented in Table 2. Aldehydes containing electron-releasing substituents like methyl, methoxy, ethoxy, isopropyl and hydroxy (**4c–4f** and **4h**) at the *para* position gave excellent yield of the corresponding xanthenes (94–97%), respectively; meanwhile, aldehydes possessing methyl and hydroxyl substituents on the *ortho* position (**4b** and **4g**) resulted in a slight drop in the yield (89% and 92%, respectively) owing to steric factors. Similarly, aldehydes containing electron-withdrawing groups such as fluoro, chloro, bromo, nitro and cyano (**4i–4k**, **4n**, and **4o**) at the *para* position gave moderate to good yield (82–91%), while the same groups present at the *ortho* (**4l**) and *meta* (**4m**) positions showed a slight drop in the yield to 84% and 87%, respectively. In the case of di-substituted aldehydes (**4p**) with methoxy groups at the *para* and *meta* positions, they also resulted in good yield (91%). Fused ring systems like naphthyl (**4q**) and aryl aldehyde substituted with a reactive functional group such as boronic acid (**4r**) underwent the reactions smoothly and gave the respective xanthene derivatives in good yields of 90% and 92%, respectively.

Next, the scope was extended to aldehydes containing heterocyclic atoms like oxygen (**4s**), which underwent the reaction readily and produced oxygen-rich xanthene derivatives in moderate yield (85%); meantime, aldehydes containing nitrogen did not give the respective xanthene. The poor or no reaction of the nitrogen-containing aldehyde is rationalised due to the coordination of the nitrogen atom with the active metal sites (Fe^{3+}) present in the catalyst, which prevents the progress of the reaction. Notably, the optimised catalytic system was also compatible with aliphatic aldehyde, which gave the corresponding product **4t** in good yield (93%). Further, to understand the efficiency of the catalyst in bulk production, the synthesis was scaled up to the one-gram scale under the identical optimised conditions, which gave excellent yield (94%) without any by-products or incomplete reaction. This scale-up also proved the efficiency of Fe(MIL-53) (**1**) MOF and present developed conditions for the industrial-scale production of xanthenes. According to the abovementioned substrate scope studies, they undoubtedly demonstrated that under the optimised conditions, the Fe(MIL-53) (**1**) MOF act as an efficient heterogeneous iron catalyst for the synthesis of a spectrum of xanthenes.

According to the screening and substrate scope studies, Fe(MIL-53) MOF (**1**) effectually catalysed the synthesis of a spectrum of xanthenes (**4a–4t**) with the minimum iron load under moderate conditions without the usage of any base, ligand or oxidant. However, to identify the role of iron present in the framework and prove its true inherent catalytic efficiency, the same xanthene synthesis was carried out using various other homogeneous iron sources under the present optimised reaction conditions, and the results are provided in Table 3. Initially, the iron source used for the synthesis of the Fe(MIL-53) MOF (**1**), iron nitrate (Table 3, entry 2), was employed as the catalyst. However, although the reaction proceeded under the optimised conditions, the yield was not impressive. A similar result was observed with other iron salts (entries 3–5, Table 3), and only poor product was produced, even after a longer reaction time (24 h). Furthermore, to understand the role of the framework metal in the synthesis of xanthene, other Lewis acid MOF catalysts were tested (Fig. 4).

Under the identical optimised reaction conditions, other transition metal-derived frameworks such as chromium [$Cr(SO_3H)$ MOF], nickel [Ni(HBTC)(BPY) MOF] and copper [$Cu_3(BTC)_2$ MOF] were tested and compared in the present xanthene synthesis. However, although all the tested MOFs catalysed the formation of xanthene, the yield is not comparable to that of Fe(MIL-53) MOF. Among the screened MOFs, the copper-based MOF $Cu_3(BTC)_2$ only gave a moderate yield (72%). Even another iron-MOF, Fe(BTC), gave only 80% of the product. This comparative study revealed the catalytic efficiency of the Fe(MIL-53) MOF (**1**) in the synthesis of xanthene. All the above-observed results from the control studies confirm that the Fe^{3+} present in the Fe(MIL-53) MOF (**1**) can efficiently catalyse the formation of xanthene derivatives. The observed results strongly evidenced that the unique characteristics of the Fe(MIL-53) MOF (**1**) such as high surface area, porous nature, and coordinatively unsaturated metal centre ligated by terephthalic acid are responsible for its high catalytic activity. Further, to prove its catalytic ability, another control experiment was performed using a 1 : 1 physical mixture of $Fe(NO_3)_3 \cdot 9H_2O$:

Table 2 Fe(MIL-53) (1) MOF-catalysed synthesis of xanthene derivatives[a]

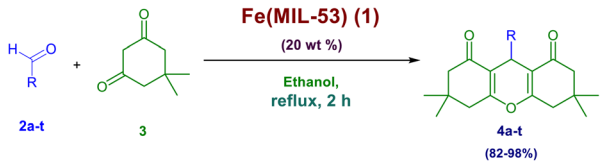

Entry	Aldehyde		Xanthene		Yield[b] (%)
1		**2a**	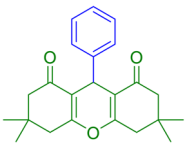	**4a**	[c]98%, 94% (Gram-scale synthesis)
2	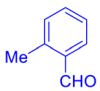	**2b**	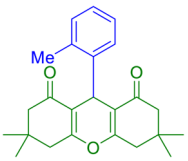	**4b**	89%
3	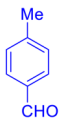	**2c**	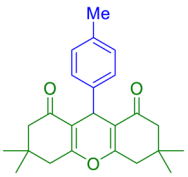	**4c**	95%
4	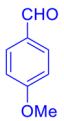	**2d**	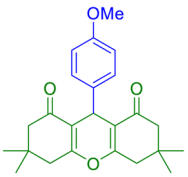	**4d**	97%
5	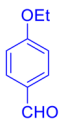	**2e**	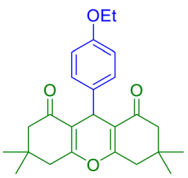	**4e**	97%
6	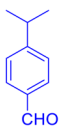	**2f**	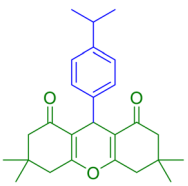	**4f**	94%
7	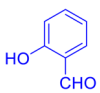	**2g**	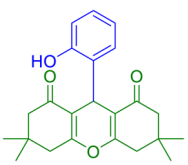	**4g**	92%
8	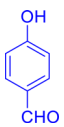	**2h**	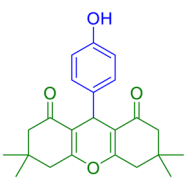	**4h**	95%

Table 2 (*Contd.*)

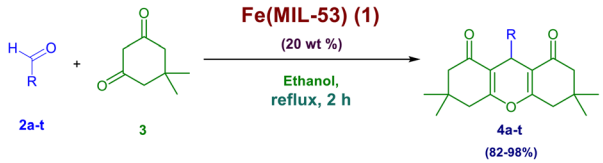

Entry	Aldehyde		Xanthene		Yield[b] (%)
9	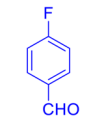	**2i**	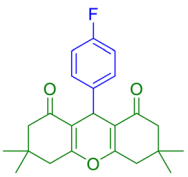	**4i**	89%
10	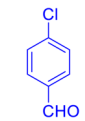	**2j**	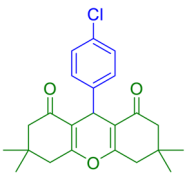	**4j**	91%
11	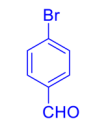	**2k**	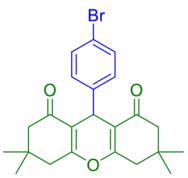	**4k**	90%
12	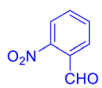	**2l**	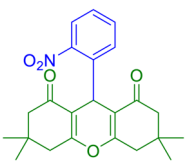	**4l**	84%
13	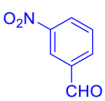	**2m**	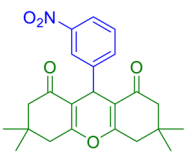	**4m**	87%
14	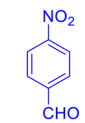	**2n**	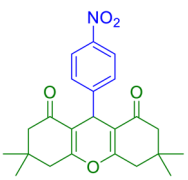	**4n**	89%
15	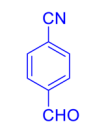	**2o**	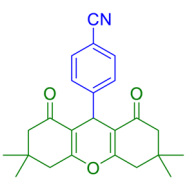	**4o**	82%
16	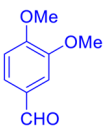	**2p**	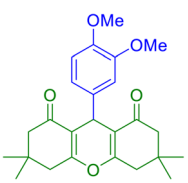	**4p**	91%

Table 2 (*Contd.*)

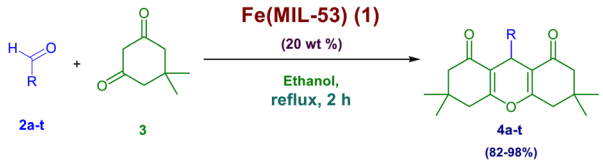

Entry	Aldehyde		Xanthene		Yield[b] (%)
17		**2q**	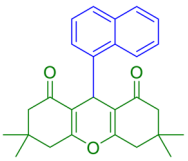	**4q**	90%
18	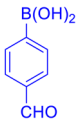	**2r**	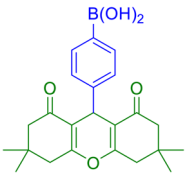	**4r**	92%
19	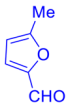	**2s**	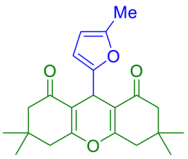	**4s**	85%
20		**2t**	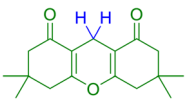	**4t**	93%

[a] Reaction conditions: aldehyde (0.71 mmol, 1.0 eq.), dimedone (1.42 mmol, 2.0 eq.), Fe(MIL-53) (20 wt%), ethanol (2.0 mL), reflux (80 °C), 2 h. [b] All are isolated yields. [c] Gram-scale synthesis.

terephthalic acid (precursors of Fe(MIL-53) MOF) as a catalyst in xanthene synthesis under the optimised conditions. The physical mixture also catalysed the reaction but only gave 17% yield. This catalytic performance of the physical mixture unambiguously confirms that the presence of the framework is responsible for the high catalytic efficiency in the synthesis of xanthene derivatives.

After successfully exploring the true catalytic efficiency of the present catalyst **1**, it was necessary to understand the stability of the heterogeneous catalyst under the screened reaction conditions, and thus hot filtration studies were carried out under the optimised conditions. During the heterogeneity test, the catalyst was removed from the reaction medium by simple filtration after 30 min under hot conditions.

Aliquots of the reaction mixture were subjected to HPLC analysis at 30 min. Extended intervals showed no further increase in the yield (Fig. 5). The hot filtration test strongly evidenced that the catalyst is highly stable and acts in a truly heterogeneous manner under the optimised reaction conditions without breaking or deforming the framework of Fe(MIL-53) (**1**). The result obtained from the hot filtration studies was strongly endorsed by the inductively coupled plasma optical emission spectroscopy (ICP-OES) measurements of the filtrate from the reaction mixture in ethanol. The catalyst was filtered from the reaction medium after 30 min, and then the filtrate was subjected to ICP-OES analysis, where no proof of iron leaching was observed, manifesting the true heterogeneity of the Fe(MIL-53) MOF (**1**).

The reusability aspect determines the stability and sustainability of a heterogeneous catalyst. This is considered one of the indispensable parameters for a reliable heterogeneous catalytic system. Due to this, the catalyst was recovered by simple filtration at the end of the reaction, dried under vacuum at 120 °C for 2 h and reused. This procedure was repeated at the end of each cycle, and the recovered catalyst was reused up to 5 times without any remarkable loss in its activity (Fig. 6). In addition, the stability of the catalyst was confirmed by subjecting the recovered catalyst to analytical confirmations such as FTIR, powder XRD and SEM.

Table 3 Effect of different iron sources in xanthene (4a) synthesis[a]

Entry	Iron source	Yield[b] (%)
1	—	—
2	$Fe(NO_3)_3 \cdot 9H_2O$	[c]22%
3	$FeCl_3$	38[c]
4	Fe_3O_4	29[c]
5	Fe(III)acac	35[c]
6	Fe(MIL-53)	98[d]

[a] Reaction conditions: catalyst (0.71 mmol), benzaldehyde (0.71 mmol, 1.0 eq.), dimedone (1.42 mmol, 2.0 eq.), ethanol (2.0 mL), reflux. [b] Isolated yield. [c] 24 h. [d] Catalyst (20 wt%).

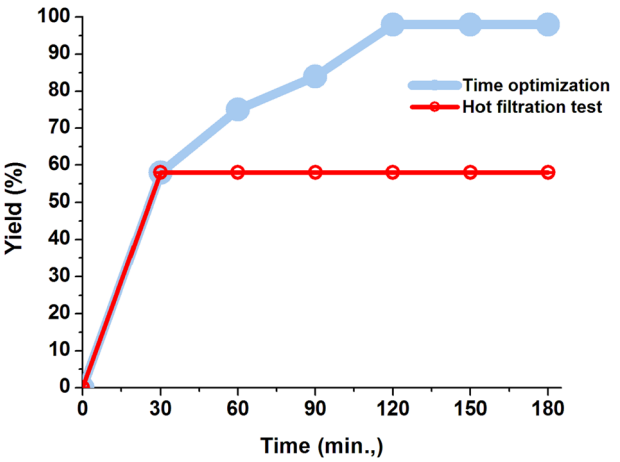

Fig. 5 Hot filtration test for understanding the true heterogeneity of Fe(MIL-53) MOF (1).

The recovered catalyst was analysed by FTIR spectroscopy before the next catalytic cycle. The FTIR analysis of the reused catalyst showed that the vibrational bands are almost identical to the as-synthesised MOF without the appearance of any new peaks, even after reusing five times. In the FTIR spectrum of Fe-MIL-53 (1) (Fig. 7), the absence of strong vibrational bands in the range of 1760–1690 cm^{-1} confirmed that the framework did not undergo any decomposition under the reaction conditions, and the carboxylate groups are still coordinated with the iron metal centre and exist as organic linkers coordinating with the secondary building units.

The observed stability results of the recovered catalyst from FTIR were further supported by the PXRD analysis. The powder XRD patterns of the recovered catalyst are identical to the fresh catalyst even after five consecutive reuses.

The presence of sharp diffraction patterns located nearly at $2\theta = 12.68°$ and 25.44° (Fig. 8) indicates that the reused MOF

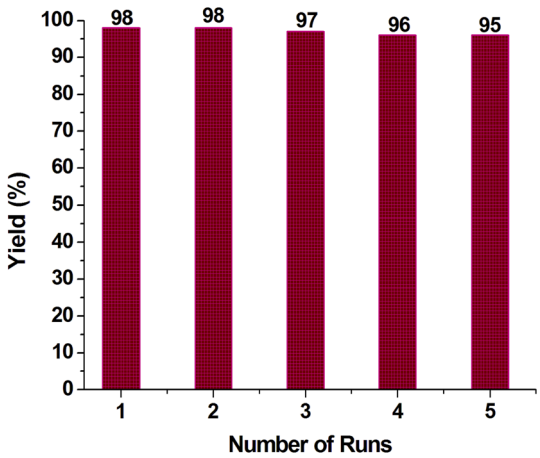

Fig. 6 Reusability profile of Fe(MIL-53) MOF (1) for the catalytic synthesis of xanthene (4a).

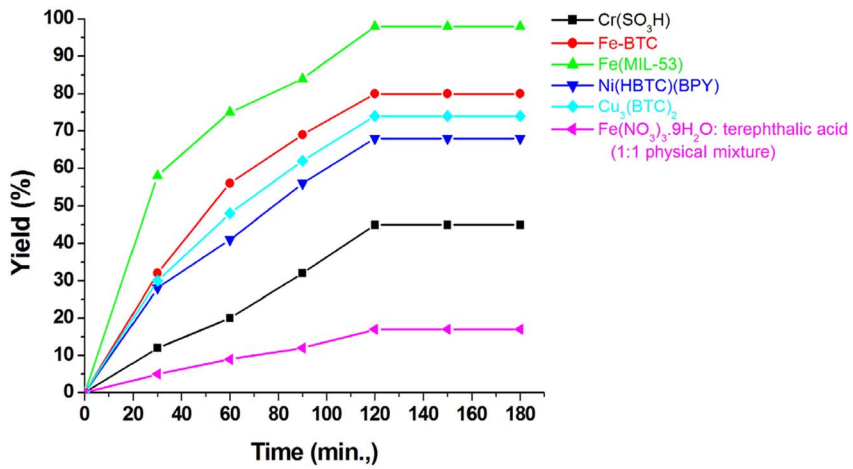

Fig. 4 Optimisation of different MOFs as catalysts for the synthesis of xanthene (4a). [a]Reaction conditions: catalyst (20 wt%), benzaldehyde (0.71 mmol, 1.0 eq.), dimedone (1.42 mmol, 2.0 eq.), ethanol (2.0 mL), reflux. Reaction monitored by HPLC.

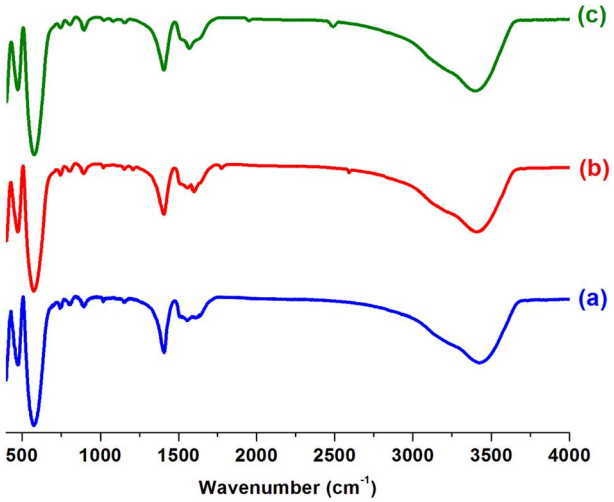

Fig. 7 FTIR spectra of fresh Fe(MIL-53) MOF (1) (a) and reused Fe(MIL-53) MOF after the second run (b) and fifth run (c).

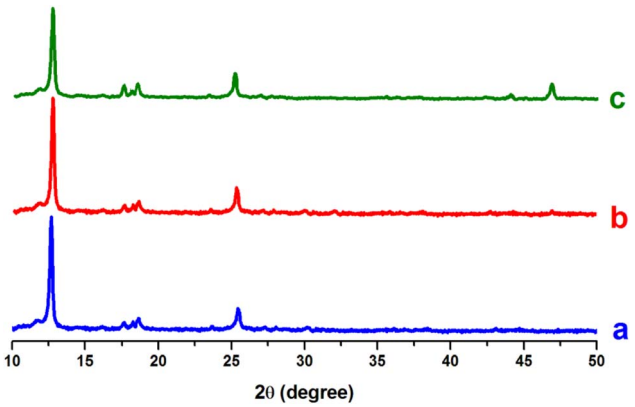

Fig. 8 Powder XRD patterns of fresh Fe(MIL-53) MOF (a) and reused Fe(MIL-53) MOF after the second run (b) and fifth run (c).

catalyst retained its crystalline nature, and the absence of any new peaks also confirmed this.

Further, the SEM analysis supports the observed stability of the reused catalyst in the PXRD analysis. The fresh Fe(MIL-53) MOF is highly crystalline in nature, with a rod-like shape and a porous and rough surface (Fig. 9). The SEM images of the reused catalyst appeared highly crystalline, and the same morphology and rod-like shape were retained in the fifth reused catalyst. This strongly disclosed that the reaction conditions, solvent and the formed products did not affect the surface morphology of the catalyst, which was responsible for retaining the catalytic efficiency of the Fe(MIL-53) MOF (**1**) even after several reuses.

All the above-mentioned analytical, experimental and reusability studies of the Fe(MIL-53) (**1**) catalyst strongly evidenced the true heterogeneity and sustainable nature of the catalyst in heterocycle synthesis. Considering this fabulous efficiency of the Fe(MIL-53) MOF (**1**), it can be employed as a catalyst for the synthesis of xanthenes.

Further, a plausible mechanism (Scheme 1) has been proposed to understand the catalytic nature based on the literature reports.[62–65] The presence of a large surface area and high density of coordinatively unsaturated open Fe^{3+} are highly responsible for the high catalytic efficiency of Fe(MIL-53) (**1**). The presence of a high density of open Fe^{3+} in the secondary building unit and its inherent Lewis acidic nature initiate the catalytic cycle. The electron-rich oxygen on the carbonyl carbon of the benzaldehyde (**2**) coordinated with the Lewis acidic Fe^{3+}, enhancing the nucleophilicity of the carbonyl carbon. The coordinated benzaldehyde (**2**) undergoes Knoevenagel condensation with a dimedone (**3**) molecule, followed by the elimination of a water molecule and an intermediate (I). After the formation of the Knoevenagel condensation intermediate, another molecule of dimedone attacks the condensed intermediate, resulting in the Michael addition product (III). Then, the intermediate (III) undergoes internal cyclisation to form (IV), which upon elimination of water, forms the desired product (**4a**) and the catalyst Fe(MIL-53) MOF (**1**) also gets regenerated and ready for another catalytic cycle.

Table 4 summarises several catalytic systems reported for the synthesis of xanthene derivatives. The peculiarity of Fe(MIL-53) MOF (**1**) is justified based on its selectivity in the synthesis of xanthenes over other existing systems, which is excellent in comparison with the other reported homogeneous and heterogeneous catalysts. The present Fe(MIL-53) MOF (**1**) exhibits enhanced catalytic activity regarding the catalyst load, reaction time, temperature and selectivity for this reaction. Furthermore, Fe(MIL-53) MOF (**1**) is highly stable, reusable, and feasible for the scaled-up synthesis of xanthenes.

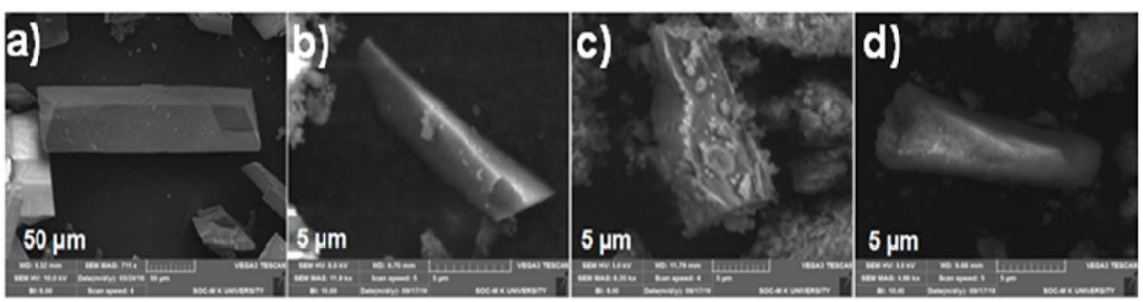

Fig. 9 SEM images of fresh (**1**) (a) and reused Fe(MIL-53) MOF after fifth run (b–d).

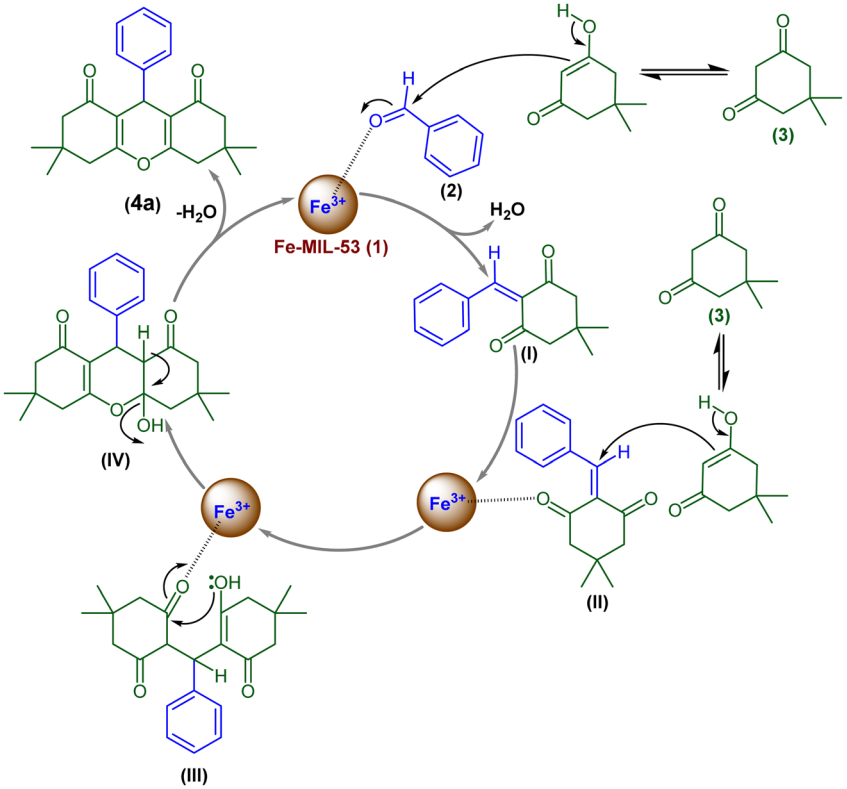

Scheme 1 Plausible mechanism for the Fe(MIL-53) MOF (**1**)-catalysed synthesis of xanthene (**4a**).

Table 4 Comparison of catalytic potential of Fe(MIL-53) MOF (**1**) in the synthesis of xanthene derivatives[a]

Entry	Catalyst	Solvent	Catalyst load	Temp (°C)	Time	Yield (%)	Reusability	Ref.
1	$FeCl_3 \cdot 6H_2O$	[bmim][BF_4]	0.1 mmol	80	6 h	92	5	18
2	Fe_3O_4 NPs	EtOH	0.1 mmol	rt	2.45 h	82	5	33[c]
3	Indium triflate [$In(CF_3SO_3)_3$]	Neat	0.02 mmol		1 h	95	5	17
4	*p*-Toluene sulfonic acid	Toluene	0.07 mmol	110	30 min	82	—	23[b]
5	Nano-Fe_3O_4–TiO_2–SO_3H (*n*-FTSA)	Neat	0.01 g	110	50 min	90	5	27
6	Fe_3O_4@NFC@NNSM-Mn(III)	EtOH	0.5 mol%	45	10 min	98	6	28[c]
7	Fe_3O_4@SiO_2@APTES@MPIB-Mn(II)	Neat	0.05 g	100	10 min	100	6	29
8	TMP-PECH-COOH polymer	Water	8 mg	50	10 min	97	6	30
9	$CuCeO_2$ NPs	Water	10 mol%	80	12 min	98	5	31
10	ZrO_2 NPs	Neat	20 mg	100	20 min	85	5	32
11	Cu(II) NPs	EtOH	0.2 g	Reflux	3.5 h	98	5	34
12	CuS quantum dots	Neat	6 mg	80	6 min	95	5	35
13	Amberlyst-15	CH_3CN	200 mg	Reflux	5 h	92	3	36
14	$NaHSO_4$	[bmim]BF_4	0.2 mmol	100	1 h	93	5	20
15	Fe-MIL(53)	EtOH	20 wt%	80 (reflux)	2 h	98	5	This work

[a] NPs-nanoparticles, 1-*n*-butyl-3-methylimidazolium tetrafluoroborate-[bmim]BF_4. [b] *N*-tosylhydrazone. [c] carboxylic acid.

3. Conclusions

In summary, a simple, facile, economical and efficient methodology for the synthesis of xanthenes was developed using an iron-based metal–organic framework Fe(MIL-53) (**1**) as a sustainable heterogeneous catalyst. The presence of coordinatively unsaturated Fe^{3+} in the secondary building unit catalyses the present heterocyclic synthesis through its inherent Lewis acidic nature. This catalyst offers a straightforward catalytic methodology to access a wide range of xanthene derivatives without any influence from the electronic nature of the substituents on aldehydes. The catalyst could be easily recovered by simple filtration and reused up to five times without any remarkable loss in its activity. The hot filtration test proved the stability and true heterogeneity of the catalyst. This Fe(MIL-53) MOF (**1**) replaces the homogeneous and non-reusable Lewis acid catalyst and acts as a solid-heterogeneous Lewis acid catalyst, replacing iron-salt-based catalysts. A

scaled-up synthesis has also been achieved effectively without significant loss in activity. To our delight, this catalyst may find broad applications in synthetic and medicinal chemistry in industry and academia. Notably, this study will open the opportunity to employ Fe(MIL-53) MOF as a potential green and sustainable alternative to homogenous iron catalysts employed in the synthesis of active pharmaceutical intermediates.

4. Experimental

4.1 General information

All reagents and starting materials were purchased commercially from Sigma-Aldrich, Alfa-Aesar, Merck, Spectrochem or CDH and used without any further purification unless otherwise noted. All ^{1}H and ^{13}C NMR spectra were recorded in $CDCl_3$ or DMSO-d_6 with TMS as an internal standard using a 300/75 MHz, 400 MHz and 500 MHz Bruker spectrometer unless otherwise noted. The powder XRD patterns of the MOF samples were recorded using a XPERT-PRO instrument using Cu Kα radiation at RT. FTIR spectra were recorded using a Shimadzu instrument in the range of 4500–500 cm^{-1}, and the samples were dispersed using the KBr pellet technique. A Netzsch Thermoanalyzer STA 409 was used for thermogravimetric analysis (TGA) at a heating rate of 10 °C min^{-1} under an N_2 atmosphere at 20–800 °C. SEM images were taken using a TESCAN VEGA3 instrument with an SE detector and equipped with an EDAX energy-dispersive X-ray spectroscopy (EDX) detector. ICP-OES measurements were performed using a PerkinElmer OPTIMA 5300 DV. HPLC analysis was carried out using a Thermo Fisher Scientific instrument using a C18 column (XBridge, 4.6 × 150) 5 μm at a flow rate of 1.0 mL min^{-1} (0.05 mol ammonium acetate buffer and acetonitrile) in the UV range of 254 nm.

4.2 Synthesis of Fe(MIL-53) MOF 1

Fe(MIL-53) was prepared according to the reported literature.[54a,66] Briefly, 4.04 g (10 mmol) of terephthalic acid, 1.66 g (10 mmol) of iron(III) nitrate nonahydrate and 100 mL of DMF were placed in a 1 L stainless steel autoclave and the temperature was maintained at 150 °C for 48 h. Then, the reaction mixture was naturally cooled to room temperature. The resulting crude Fe(MIL-53) was recovered as an orange solid by filtration. Further, the resulting orange crystals were washed with DMF followed by acetone and dried in air. The resulting dry solid was further super dried at 100 °C under vacuum in a Buchi® glass oven for 8 h, yielding 1.60 g (94%) of Fe(MIL-53) metal–organic framework as a brown solid with respect to 1,4-benzenedicarboxylic acid.

The resulting Fe(MIL-53) MOF (**1**) crystals were characterised using FTIR, PXRD, TGA, SEM and elemental analysis (ICP-OES and EDAX). In the powder XRD pattern, the presence of the very sharp peaks located nearly at $2\theta = 12.68°$ and 25.44° (Fig. S2) indicates that the MOF was highly crystalline in nature, and the observed pattern exactly matches the reported and simulated patterns.[67] The FTIR spectrum of Fe(MIL-53) exhibits the absence of strong vibrational bands at 1760–1690 cm^{-1}, which confirmed the deprotonation of the carboxylic acid groups in 1,4-benzenedicarboxylic acid. As shown in Fig. S1, the characteristic peaks were located at 576, 743, 1406 and 1553 cm^{-1} in its infrared spectrogram, providing evidence for the presence of –COOFe metallic esters in MIL-53(Fe). The bands at 744, 809 and 893 cm^{-1} are due to the existence of the C–CO_2 bond.[45] TGA showed that Fe(MIL-53) exhibited good stability, which is in good agreement with the previous studies. The freshly synthesised Fe(MIL-53) exhibited the initial weight loss at approximately 100 °C due to the evaporation of acetone and guest water molecules present inside the MOF pores. After that, there was a gradual weight loss up to 310 °C due to evaporation of coordinated DMF solvent in the pores of the MOF. Further, the material began to decompose at 310 °C, which indicates that the Fe(MIL-53) MOF is stable up to 300 °C. According to the ICP-OES data, the iron loading was found to be about 0.124 mmol g^{-1} (6.93% of iron), which is consistent with the EDAX measurement. The SEM micrograph of the Fe(MIL-53) MOF shows a crystalline morphology with rod-like shape, which is in good agreement with the literature.[68] The overall analysis of the prepared Fe(MIL-53) MOF is well supported by the reported results.

4.3 General procedure for Fe(MIL-53)-catalyzed synthesis of xanthenes

A mixture of aldehyde (0.71 mmol, 1.0 eq.) and dimedone (1.42, 2.0 eq.) was dissolved in 3.0 mL of ethanol in an oven-dried glass vessel with a magnetic stir bar and placed in an oil bath. Then 20 wt% of Fe(MIL-53) MOF (**1**) catalyst was added to the reaction mixture and stirred under reflux conditions (80 °C) for 2 h. The course of the reaction was monitored by TLC. Upon completion of the reaction, the reaction mixture was cooled to room temperature. Then, the catalyst was separated and recovered by a simple filtration. Further, the catalyst was repeatedly washed with ethanol to remove the products present inside the pores of the MOF. The combined organic layer was evaporated to dryness under vacuum, and the crude product was purified by passing through silica gel (60–120 mesh) using 9 : 1 petroleum ether and ethyl acetate as the eluent, which yielded the pure product. All the purified compounds were characterised by ^{1}H and ^{13}C spectroscopy. The recovered catalyst was washed with chloroform and dried in a glass oven at 120 °C. After drying, it was analysed by FTIR, PXRD and SEM to confirm its original structure for further use.

Author contributions

Ganesapandian Latha-conceptualization, methodology, analytical data curation, original writing, data validation. Natarajan Saravanakumar-writing, data validation. Nainamalai Devarajan-methodology, writing. Kamaraj Shivaranjan-data curation. Data validation. Palanisamy Suresh-conceptualization, methodology, writing and review, data validation, funding, resource management.

Conflicts of interest

There are no conflicts to declare.

Data availability

All the data from the research article are available in the SI. See DOI: **https://doi.org/10.1039/d5su00191a**.

Acknowledgements

Dr PS acknowledge the financial support from Madurai Kamaraj University-Rashtriya Uchchatar Shiksha Abhiyan (MKU-RUSA 2.0) (007-R2/MKU/SOC/2020-2021 for GC-MS), Tamil Nadu State Council for Higher Education (TANCSHE) (131/2019A), Tamil Nadu State Council for Science and Technology (TNSCST/STP/Covid-19/2020-21-3682), Science and Engineering Research Board SERB), New Delhi, (SR/FT/CS-53/2011) and CSIR, New Delhi. Department of Science and Technology Fund for Improvement of S&T Infrastructure in Universities (DST-FIST) (for 400 MHz NMR) (SR/FST/CS-II/2017/35(C)) and University Grants Commission under University with Potential for Excellence program (UGC-UPE), DST-PURSE (for FTIR, SEM, and EDX) are acknowledged for the instrumental facilities. GL thank UGC Non-NET fellowship XII plan scheme.

References

1 N. Mulakayala, P. V. N. S. Murthy, D. Rambabu, M. Aeluri, R. Adepu, G. R. Krishna, C. M. Reddy, K. R. S. Prasad, M. Chaitanya, C. S. Kumar, M. V. B. Rao and M. Pal, *Bioorg. Med. Chem. Lett.*, 2012, **22**, 2186.
2 K. R. M. Naidu, B. S. Krishna, M. A. Kumar, P. Arulselvan, S. I. Khalivulla and O. Lasekan, *Molecules*, 2012, **17**, 7543.
3 A. G. Banerjee, L. P. Kothapalli, P. A. Sharma, A. B. Thomas, R. K. Nanda, S. K. Shrivastava and V. V. Khatanglekar, *Arab. J. Chem.*, 2016, **9**, S480.
4 A. Barmaka, K. Niknam, G. Mohebbi and H. Pournabi, *Microb. Pathog.*, 2019, **130**, 95.
5 J. R. Kim and S. Michielsen, *Nanomater.*, 2016, **6**, 243.
6 S. Zukića and U. Maran, *SAR QSAR Environ. Res.*, 2020, **31**, 905.
7 M. Abualhasan, M. Hawash, S. Aqel, M. Al-Masri, A. Mousa and L. Issa, *ACS Omega*, 2023, **8**, 37623.
8 (*a*) H. A. Soliman and T. A. Salama, *Chin. Chem. Lett.*, 2013, **24**, 404; (*b*) R. Shashi and N. S. Begum, *Phosphorus Sulfur Silicon Relat. Elem.*, 2022, **197**, 38.
9 (*a*) S. A. Hilderbrand and R. Weissleder, *Tetrahedron Lett.*, 2007, **48**, 4383; (*b*) I. Rajapaksha, H. Chang, Y. Xiong, S. Marder, S. R. Gwaltney and C. N. Scott, *J. Org. Chem.*, 2020, **85**, 12108.
10 (*a*) I. Devi and P. J. Bhuyan, *Tetrahedron Lett.*, 2004, **45**, 8625; (*b*) L. G. Rivero, J. Bañuelos and I. L. Arbeloa, *Int. Rev. Phys. Chem.*, 2015, **34**, 515.
11 G. Pohlers, R. Sinta and J. C. Scaiano, *Chem. Mater.*, 1997, **9**, 3222.
12 (*a*) C. G. Knight and T. Stephens, *Biochem. J.*, 1989, **258**, 683; (*b*) S. G. Keller, M. Kamiya and Y. Urano, *Molecules*, 2020, **25**, 5964.
13 M. Gosi, A. C. Kumar and Y. Sunandamma, *J. Fluoresc.*, 2022, **32**, 2379.
14 (*a*) H. J. Timpe, S. Ulrich, C. Decker and J. P. Fouassier, *Macromolecules*, 1993, **26**, 4560; (*b*) K. M. Khan, G. M. Maharvi, M. T. H. Khan, A. J. Shaikh, S. Perveen, S. Begum and M. I. Choudhary, *Bioorg. Med. Chem.*, 2006, **14**, 344.
15 F. Darviche, S. Balalaie, F. Chadegani and P. Salehi, *Synth. Commun.*, 2007, **37**, 1059.
16 (*a*) X. Fan, X. Hu, X. Zhang and J. Wang, *Can. J. Chem.*, 2005, **83**, 16; (*b*) G. K. Verma, K. Raghuvanshi, R. K. Verma, P. Dwivedi and M. S. Singh, *Tetrahedron*, 2011, **67**, 3698.
17 B. Karami, K. Eskandari and G. Ansari, *Der Chemica Sinica*, 2017, **8**, 342–354.
18 X.-S. Fan, Y.-Z. Li, X.-Y. Zhang, X.-Y. Hu and J.-J. Wang, *Chin. J. Org. Chem.*, 2005, **25**, 1482.
19 D. Pavithra and K. R. Ethiraj, *Polycyclic Aromat. Compd.*, 2022, **42**, 1078.
20 J.-J. Ma, J.-C. Li, R.-X. Tang, X. Zhou, Q. H. Wu, C. Wang, M. M. Zhang and Q. Li, *Chin. J. Org. Chem.*, 2007, **27**, 640.
21 G. I. Shakibaei, P. Mirzaei and A. Bazgir, *Appl. Catal. A., Gen.*, 2007, **325**, 188.
22 A. John, P. J. P. Yadav and S. Palaniappan, *J. Mol. Catal. A: Chem.*, 2006, **248**, 121.
23 D. Choudhary, C. Agrawal, V. Khatri, R. Thakuria and A. K. Basak, *Tetrahedron Lett.*, 2017, **58**, 1132.
24 R. S. Salama, S. M. El-Bahy and M. A. Mannaa, *Colloids Surf., A*, 2021, **628**, 127261.
25 S. Kantevari, R. Bantu and L. Nagarapu, *J. Mol. Catal. A: Chem.*, 2007, **269**, 53.
26 T. S. Jin, J. S. Zhang, A. Q. Wang and T. S. Li, *Synth. Commun.*, 2005, **35**, 2339.
27 A. Amoozadeh, S. Golian and S. Rahmani, *RSC Adv.*, 2015, **5**, 45974.
28 P. G. Kargar, G. Bagherzade and H. Eshghi, *RSC Adv.*, 2021, **11**, 4339.
29 A. Karimian, M. Norouzi, A. Ebrahimnia and A. Nozari, *J. Mol. Struct.*, 2024, **1297**, 137014.
30 K. Hiba, M. Shaibuna, S. Prathapan and K. Sreekumar, *ChemistrySelect*, 2021, **6**, 13832.
31 S. A. Shaikh, V. S. Kamble, S. T. Salunkhe, S. K. Patil and B. D. Aghav, *Org. Prep. Proced. Int.*, 2023, **55**, 393.
32 P. Bansal, N. Kaur, C. Prakash and G. R. Chaudhary, *Vacuum*, 2018, **157**, 9.
33 (*a*) M. A. Ghasemzadeh, J. S. -Ghomi and S. Zahedi, *J. Serb. Chem. Soc.*, 2013, **78**, 769; (*b*) D. Thirumalai and S. Gajalakshmi, *Res. Chem. Intermed.*, 2020, **46**, 2657.
34 A. Amini, A. Fallah, C. Cheng and M. Tajbakhsh, *RSC Adv.*, 2018, **8**, 41536.
35 P. Bansal, G. R. Chaudhary, N. Kaur and S. K. Mehta, *RSC Adv.*, 2015, **5**, 8205.
36 B. Das, P. Thirupathi, I. Mahender, V. S. Reddy and Y. K. Rao, *J. Mol. Catal. A: Chem.*, 2006, **247**, 233.

37 (*a*) G. Harichandran, S. D. Amalraj and P. Shanmugam, *J. Mol. Catal. A: Chem.*, 2014, **392**, 31; (*b*) N. Devarajan, M. Karthik and P. Suresh, *Org. Biomol. Chem.*, 2017, **15**, 9191.
38 (*a*) T. Zhang and W. B. Lin, *Chem. Soc. Rev.*, 2014, **43**, 5982; (*b*) D. Li, A. Yadav, H. Zhou, K. Roy, P. Thanasekaran and C. Lee, *Global Chall.*, 2024, **8**, 2300244; (*c*) S. Thakur and S. Bharti, *J. Inorg. Organomet. Polym. Mater.*, 2024, **34**, 4477–4508.
39 (*a*) M. R. -Torrente, L. D. B. Mandemaker, M. Filez, G. Delen, B. Seoane, F. Meirer and B. M. Weckhuysen, *Chem. Soc. Rev.*, 2020, **49**, 6694; (*b*) N. Devarajan and P. Suresh, *Org. Chem. Front.*, 2018, **5**, 2322; (*c*) G. Latha, N. Devarajan, M. Karthik and P. Suresh, *Catal. Commun.*, 2020, **136**, 105911.
40 (*a*) Y. Lin, C. Kong and L. Chen, *RSC Adv.*, 2016, **6**, 32598; (*b*) L. Zhu, X.-Q. Liu, H.-L. Jiang and L.-B. Sun, *Chem. Rev.*, 2017, **117**, 8129; (*c*) N. Devarajan, N. Saravanakumar and P. Suresh, *Appl. Organomet. Chem.*, 2025, **39**, e70031; (*d*) Z. Sharifzadeh and A. Morsali, *Coord. Chem. Rev.*, 2022, **459**, 214445.
41 (*a*) J. Jiang and O. M. Yaghi, *Chem. Rev.*, 2015, **115**, 6966; (*b*) N. Devarajan and P. Suresh, *New J. Chem.*, 2019, **43**, 6806; (*c*) W. Gong, Y. Liu, H. Li and Y. Cui, *Coord. Chem. Rev.*, 2020, **420**, 213400; (*d*) P. Leo, N. Crespí, C. Palomino, A. Martín, G. Orcajo, G. Calleja and F. Martinez, *Catal. Today*, 2022, **258**, 390–391.
42 (*a*) A. Corma, H. García and F. X. Llabrés i Xamena, *Chem. Rev.*, 2010, **110**, 4606; (*b*) A. Dhakshinamoorthy and H. Garcia, *Chem. Soc. Rev.*, 2012, **41**, 5262; (*c*) N. Devarajan and P. Suresh, *ChemCatChem*, 2016, **8**, 2953; (*d*) G. Latha, N. Devarajan and P. Suresh, *ChemistrySelect*, 2020, **5**, 10041.
43 (*a*) C. Jiang, X. Wang, Y. Ouyang, K. Lu, W. Jiang, H. Xu, X. Wei, Z. Wang, F. Dai and D. Sun, *Nanoscale Adv.*, 2022, **4**, 2077; (*b*) L.-T. Zhang, Y. Zhou and S.-T. Han, *Angew. Chem., Int. Ed.*, 2021, **133**, 15320; (*c*) J. Yang and Y.-W. Yang, *Small*, 2020, **16**, 1906846.
44 (*a*) K. Wang, D. Feng, T. F. Liu, J. Su, S. Yuan, Y. P. Chen, M. Bosch, X. Zou and H. C. Zhou, *J. Am. Chem. Soc.*, 2014, **136**, 13983; (*b*) L. Hanna, P. Kucheryavy, C. Liu, X. Zhang and J. V. Lockard, *J. Phys. Chem. C*, 2017, **121**, 13570; (*c*) A. Ramirez, L. Gevers, A. Bavykina, S. O. -Chikh and J. Gascon, *ACS Catal.*, 2018, **8**, 9174; (*d*) D. Lv, H. Wang, Y. Chen, F. Xu, R. Shi, Z. Liu, X. Wang, S. J. Teat, Q. Xia, Z. Li and J. Li, *ACS Appl. Mater. Interfaces*, 2018, **10**, 6031.
45 N. Devarajan and P. Suresh, *Asian J. Org. Chem.*, 2020, **9**, 437.
46 (*a*) F. Zhang, J. Shi, Y. Jin, Y. Fu, Y. Zhong and W. Zhu, *Chem. Eng. J.*, 2015, **259**, 183; (*b*) N. E. Elharony, I. El T. El Sayed, A. G. Al-Sehemi, A. A. Al-Ghamdi and A. S. A. -Elyazed, *Catalysts*, 2021, **11**, 1451.
47 S. Tomar and V. K. Singh, *Mater. Today Proc.*, 2021, **43**, 3291.
48 (*a*) J. Tang, M. Yang, M. Yang, J. Wang, W. Dong and G. Wang, *New J. Chem.*, 2015, **39**, 4919; (*b*) S. Edebali, *Appl. Surf. Sci. Adv.*, 2023, **18**, 100496.
49 (*a*) S. Bauer, C. Serre, T. Devic, P. Horcajada, J. Marrot, G. Ferey and N. Stock, *Inorg. Chem.*, 2008, **47**, 7568; (*b*) M. Almáši, V. Zeleňák, P. Palotai, E. Beňová and A. Zeleňáková, *Inorg. Chem. Commun.*, 2018, **93**, 115.
50 (*a*) Y. Yang, B. Li, D. Fu, J. Chen, S. Cui, X. He, K. Liu, S. Wei, D. Li and Q. Han, *Green Chem.*, 2023, **25**, 8093; (*b*) S. H. Doan, C. B. Tran, A. L. N. Cao, N. T. H. Le and N. T. S. Phan, *Catal. Lett.*, 2019, **149**, 2053.
51 (*a*) S. H. Doan, K. D. Nguyen, P. T. Huynh, T. T. Nguyen and N. T. S. Phan, *J. Mol. Catal. A: Chem.*, 2016, **423**, 433; (*b*) S. H. Doan, K. D. Nguyen, T. T. Nguyen and N. T. S. Phan, *RSC Adv.*, 2017, **7**, 1423.
52 (*a*) T. N. Lieu, K. D. Nguyen, D. T. Le, T. Truong and N. T. S. Phan, *Catal. Sci. Technol.*, 2016, **6**, 5916; (*b*) H. T. Dang, T. N. Lieu, T. Truong and N. T. S. Phan, *J. Mol. Catal. A: Chem.*, 2016, **420**, 237.
53 (*a*) S. H. Doan, V. H. H. Nguyen, T. H. Nguyen, P. H. Pham, N. N. Nguyen, A. N. Q. Phan, T. N. Tu and N. T. S. Phan, *RSC Adv.*, 2018, **8**, 10736; (*b*) V. H. H. Nguyen, S. H. Doan, T. T. Van, P. H. Pham, T. T. N. Nguyen, N. N. Nguyen, T. N. Tu and N. T. S. Phan, *Appl. Organomet. Chem.*, 2019, **33**, e4841.
54 (*a*) P. Horcajada, C. Serre, G. Maurin, N. A. Ramsahye, F. Balas, M. V. -Regi, M. Sebban, F. Taulelle and G. Ferey, *J. Am. Chem. Soc.*, 2008, **130**, 6774; (*b*) H. P. N. Thi, H. D. Ninh, C. V. Tran, B. T. Le, S. V. Bhosale and D. D. La, *ChemistrySelect*, 2019, **4**, 2333.
55 (*a*) R. Panda, S. Rahut and J. K. Basu, *RSC Adv.*, 2016, **6**, 80981; (*b*) C. M. Navarathna, N. B. Dewage, A. G. Karunanayake, E. L. Farmer, F. Perez, E. L. B. Hassan, T. E. Mlsna, C. U. Pittman Jr. and J. Inorg, *Organomet. Polym.*, 2020, **30**, 214.
56 (*a*) L. Ai, L. Li, C. Zhang, J. Fu and J. Jiang, *Chem.–Eur. J.*, 2013, **19**, 15105; (*b*) X. Yi, W. Dong, X. Zhang, J. Xie and Y. Huang, *Anal. Bioanal. Chem.*, 2016, **408**, 8805.
57 P. D. Du and P. N. Hoai, *Adv. Mater. Sci. Eng.*, 2021, **2021**, 5540344.
58 M. A. Ghasemzadeh, B. M. -Eshkevari and M. H. A. Basir, *Appl. Organometal. Chem.*, 2019, **33**, 4679.
59 A. Nozarie, *Chem. Methodol.*, 2019, **3**, 704.
60 M. H. A. -Basir, F. Shirini, H. Tajik and M. A. Ghasemzadeh, *J. Mol. Struct.*, 2019, **1197**, 318.
61 D. Prat, J. Hayler and A. Wells, *Green Chem.*, 2014, **16**, 4546.
62 A. Ilangovan, S. Muralidharan, P. Sakthivel, S. Malayappasamy, S. Karuppusamy and M. P. Kaushik, *Tetrahedron Lett.*, 2013, **54**, 491.
63 N. Patel, D. Katheriya, H. Dadhania and A. Dadhania, *AIP Conf. Proc.*, 2018, **1961**, 030011.
64 A. N. Dadhania, V. K. Patel and D. K. Raval, *C. R. Chim.*, 2012, **15**, 378–383.
65 A. N. Dadhania, V. K. Patel and D. K. Raval, *J. Saudi Chem. Soc.*, 2014, **21**, S163–S169.
66 (*a*) C. Scherb, A. Schodel and T. Bein, *Angew. Chem.*, 2008, **120**, 5861; (*b*) C. Zhang, L. Ai and J. Jiang, *J. Mater. Chem. A*, 2015, **3**, 3074.
67 R. Liang, F. Jing, L. Shen, N. Qin and L. Wu, *J. Hazard. Mater.*, 2015, **287**, 364.
68 N. T. Nguyen, X. T. Nguyen, D.-T. Nguyen, H. M. Tran, T. M. Nguyen and T. Q. Tran, *Adsorpt. Sci. Technol.*, 2021, **2021**, 5906248, DOI: **10.1155/2021/5906248**.